University of Reading

Numerical Schemes Applied to the Burgers and Buckley-Leverett Equations

by

Rakib Ahmed

September 2004

Department of Mathematics

———————————————————————————

Submitted to the Department of Mathematics, University of Reading, in partial fulfilment of the requirements for the Degree of Master of Science.

Acknowledgements

I would like to thank my supervisor Professor Mike Baines for his support and patience throughout the duration of this dissertation. I would also like to thank Dr Peter Sweby, Mark Wakefield, Paul Jelfs, Sue Davis and the postgraduate students in the department, for their assistance and encouragement.

Many thanks also go to the EPSRC for the scholorship which enabled the financial support throughtout this course.

Finally I would like to thank my family and friends for their love and support.

Declaration

I confirm that this is my own work and the use of all materials from other sources has been properly and fully acknowledged.

Signed

Contents

1 Introduction 6

2 Exact Solution by Characteristics 9

2.1 Burgers' Equation 10

2.1.1 Entropy Condition 11

2.1.2 Initial Data 1 12

2.1.3 Initial Data 2 14

2.2 Buckley-Leverett Equation 18

2.2.1 Initial Data 1 for the B-L equation 19

2.2.2 Initial Data 2 for the B-L equation 21

3 Classical numerical schemes 24

3.1 The CFL condition 25

3.2 Lax-Friedrichs 26

3.3 First order upwind 28

3.4 Lax-Wendro 31

3.5 Warming-Beam 33

3.6 TVD and Limiters 34

3.7 Modified Equation 35

4 Discontinuous Galerkin Method 38

4.1 Basic derivation of D-G Method 38

4.2 Buckley-Leverett flux 41

5 Numerical Results 46

5.1 Burgers initial data 1 47

5.2 Burgers initial data 2 49

5.3 Buckley - Leverett initial data 1 52

5.4 Buckley - Leverett initial data 2 54

6 Conclusion 57

6.1 Further work 58

Chapter 1

Introduction

Consider the hyperbolic conservation law

$$u_t + f(u)_x = 0 \tag{1.1}$$

where u is the conserved quantity and $f(u)$ is the flux. Applications of such equation

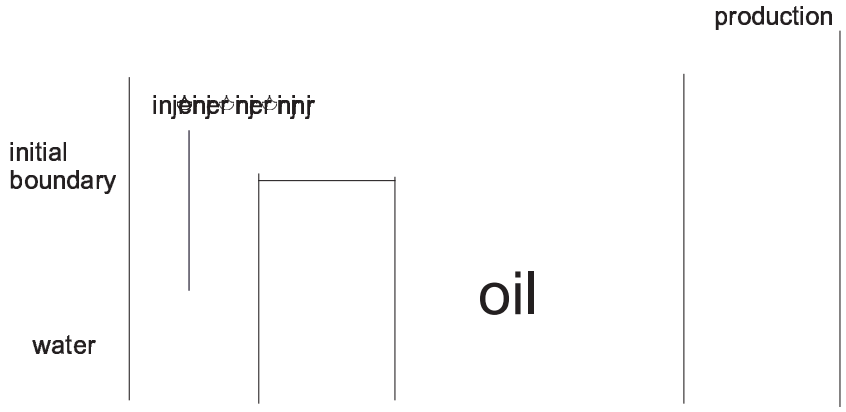

Figure 1.1: Sketch to show the basic technique

The Buckley-Leverett equation is used for oil recovery in industry. The discovery and recovery of oil is highly complex process, in which mathematical modelling and numerical simulation play a crucial role. Usually when an oil well is produced, the pressure at early stage is naturally high, and is such that there will be minimum di□culty in recovering the oil. The rate at which oil flows out of the well will naturally diminish with time; common ways of keeping up the oil flowing is to inject water to drive the oil towards the producing well.

Generally an oil reservoir consists of layers of porous rock, which are sandwiched between layers of impervious rock. These layers are often bent up in a cup shape which is known as an anticline. The oil reservoir is formed when oil is produced over geological time scales at great depths, migrating into a reservoir which is filled with water. This movement causes displacement to the water; gas may also be present depending on the pressure conditions. If gas is

Chapter 2

Exact Solution by Characteristics

Consider the hyperbolic conservation law

$$u_t + f(u)_x = 0 \tag{2.1}$$

where $f(u)$ is the flux function. This can also be written as

$$u_t + a(u)u_x = 0$$

where

$$a(u) = f^0(u):$$

A basic solution procedure for hyperbolic equations is the method of characteristics, which will allow us to investigate the features of the solution of this equation. The characteristics are given by

$$\frac{dx}{dt} = a(u); \ \ on \ which \ \frac{du}{dt} = 0 \tag{2.2}$$

We can see that on the characteristics

$$\overline{dt}$$

The characteristics are given by equation 2

Figure 2.1: To show the shape of Burgers' equation

Here

$$f(u) = \frac{1}{2}u^2 \qquad and \qquad a(u) = u$$

where $f(u)$ has a convex shape (see Fig. 2.2). Then

2.1.2 Initial Data 1

We first use the initial data (in the right half of the plane)

$$u(x;0) = \begin{cases} \frac{1}{2} & x = 0 \\ 0 & x > 0 \end{cases} \qquad 8t$$

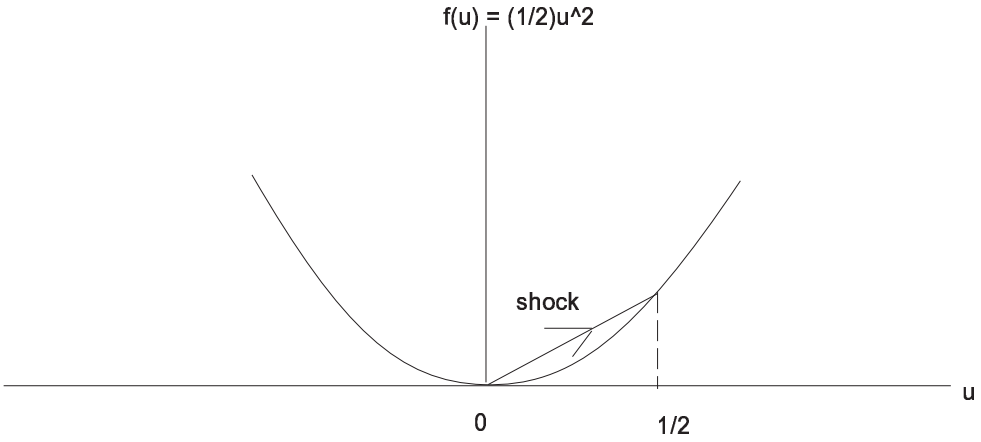

Figure 2.2: Shape of $f(u)$ for Burgers' equation with initial data 1 points

The characteristics are given by

$$\frac{du}{dt} = 0; \qquad \frac{dx}{dt} = u \;) \begin{cases} u = u_0 \\ x = u_0 t + x_0 & (\textit{leaving the } x \text{ ¡ } \textit{axis}) \\ x = u_0(t \text{ ¡ } t_0) & (\textit{leaving the } t \text{ ¡ } \textit{axis}) \end{cases} \qquad (2.7)$$

Here

$$\frac{dx}{dt} = \begin{cases} \\ \\ \end{cases}$$

until they cross. Integrating equation (2:8), we obtain

$$x = \begin{cases} \frac{1}{2}\left(t - t_0\right)^2 & \text{when} \quad t > 0; \quad x > 0 \\ x_0 & \text{when} \quad x > 0; \quad t > 0 \end{cases} \tag{2.9}$$

which agrees with equation (2:4). We can clearly see that the characteristics initially cross at $x = 0$ when $t = 0$. Therefore at the time t

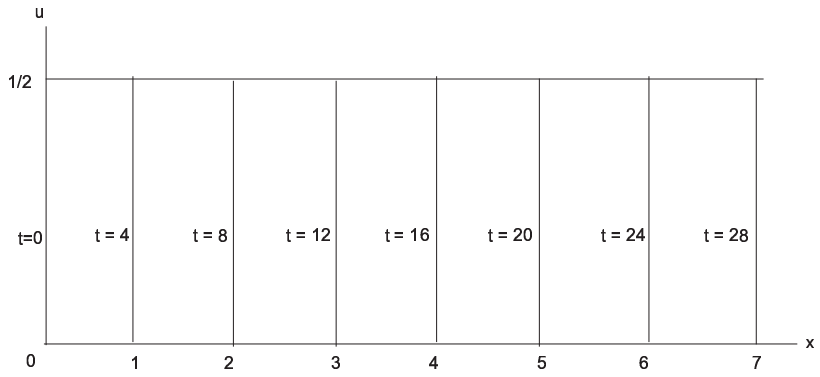

Figure 2.4: Graph to show solution at intervals of t =4, for example 1

2.1.3 Initial Data 2

Secondly we use the initial data (on the whole x-axis)

$$u(x;0) = \begin{cases} 0 & x < \ _i 1 \\ \frac{1}{2} & \ _i 1 < x < 0 \\ 0 & x > 0 \end{cases}$$

To evaluate the characteristics in the x,t plane for all $t > 0$, we proceed as follows.

The characteristics are given by

$$\frac{du}{dt} = 0; \qquad \frac{dx}{dt} = u_0 = \begin{cases} 0 & x_0 : 0 \\ \end{cases}$$

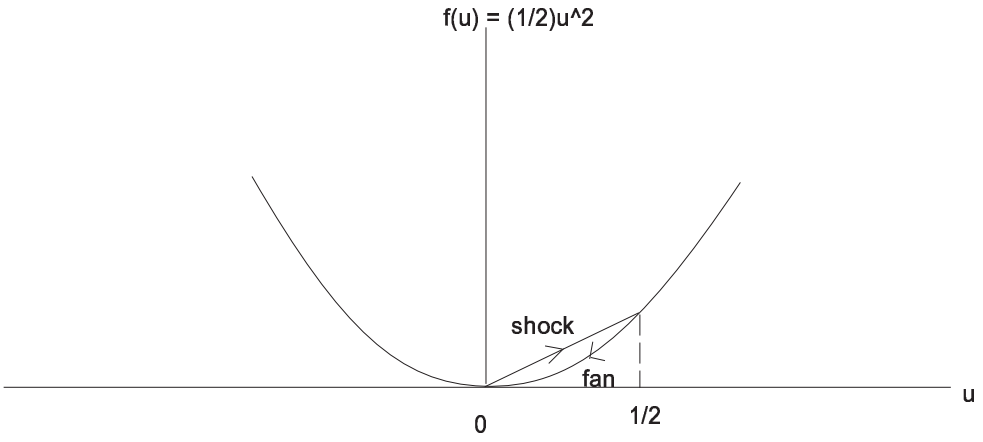

Figure 2.5: Flux function for Burgers' equation with initial data 2 points

i.e

$$\frac{dx}{dt} = \begin{cases} 0 & u = 0 \quad for \quad x < -1; \quad t > 0: \\ \frac{1}{2} & u = \frac{1}{2} \quad for \quad t > 0 \quad -1 \le x \le 0 \\ 0 & u = 0 \quad for \quad x > 0; \quad t > 0: \end{cases} \tag{2.13}$$

until they cross. Integrating equation (2:13), we obtain

$$x = \begin{cases} x_0 & when \quad x < -1; \quad t > 0 \\ \frac{1}{2}\, t - t_0 & when \quad -1 \le x \le 0; \quad t > 0 \\ x_0 & when \quad x > 0; \quad t > 0 \end{cases} \tag{2.14}$$

The shock is initially at $x = 0$. We proceed as follows to calculate the shock speed. As before

$$S = \frac{[f]}{[u]} = \frac{f_R - f_L}{u_R - u_L} = \frac{\frac{1}{2}(0)^2 - \frac{1}{2}\frac{1}{2}^2}{0 - \frac{1}{2}} = \frac{1}{4} \tag{2.15}$$

Connecting $(0; 0)$ to $(0; \frac{1}{2})$ is a straight line which represents the shock. By looking

at Figure (2.5) we can visualise that by connecting $\frac{1}{2}$ to 0 on the curve represents the fan. The initial shock for this problem is at $x = 0$ with a speed which is $\frac{1}{4}$. Using this we obtain the shock line $x_s($ $_s$

Hence for $t \cdot 4$ we have

$$u(x;t) = \begin{cases} 0 & x < -1 \\ \frac{x+1}{t} & -1 < x < \frac{t}{2} - 1 \\ \frac{1}{2} & \frac{t}{2} - 1 < x < \frac{1}{4}t \\ 0 & \frac{1}{4}t < x \end{cases} \tag{2.18}$$

(see Figure 2.6). We now look at the form of the shock when the expansion meets

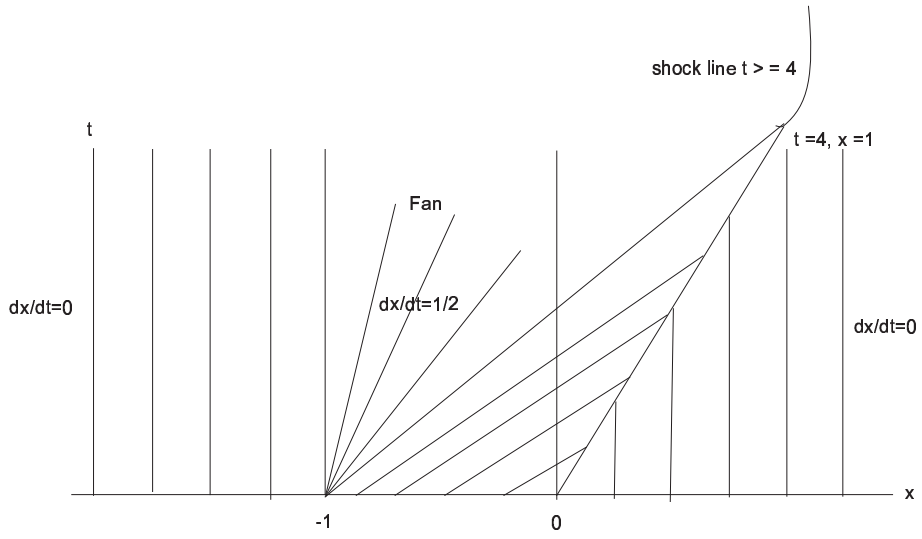

Figure 2.6: Burgers' equation for example 2

the shock $t \geq 4$. To do this we equate the shock speed to the average of the values to the left and to the right:

$$\frac{dx_s}{dt} = \frac{1}{2}\left(u_R + u_L\right) = \frac{1}{2}\left(\frac{(x_s+1)}{t} + 0\right)$$

i.e.

$$S = \frac{dx_s}{dt} = \frac{(x_s+1)}{2t} \tag{2.19}$$

From equation (2:16) we can see that the ODE is separable, giving rise to

$$\int \frac{dx_s}{}$$

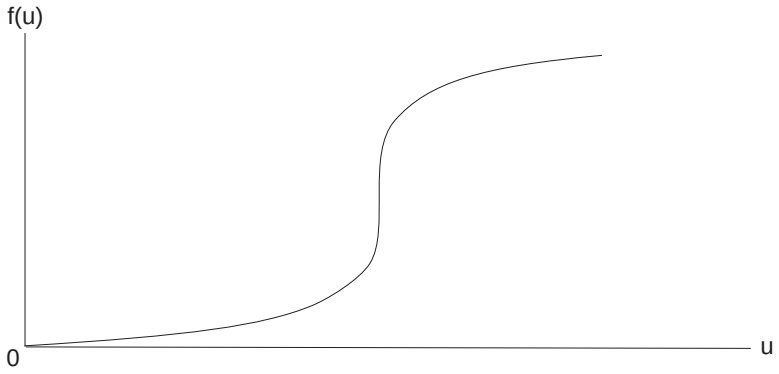

Figure 2.7: To show the shape of a non-convex function

2.2.1 Initial Data 1 for the B-L equation

In this problem we will again use the initial data

$$u(x;0) = \begin{cases} \frac{1}{2} & x = 0 \\ 0 & x > 0 \end{cases}$$

To evaluate the characteristics in the x,t plane for all $t > 0$, we proceed as follows. The characteristics are given by

$$\frac{dx}{dt} = a(u); \qquad \frac{du}{dt} = 0 \tag{2.23}$$

We can see that u is a constant which shall be denoted by u_0. From equation (2:23), $u = u_0$ and x is given by

$$x = a(u_0)t + x_0 \tag{2.24}$$

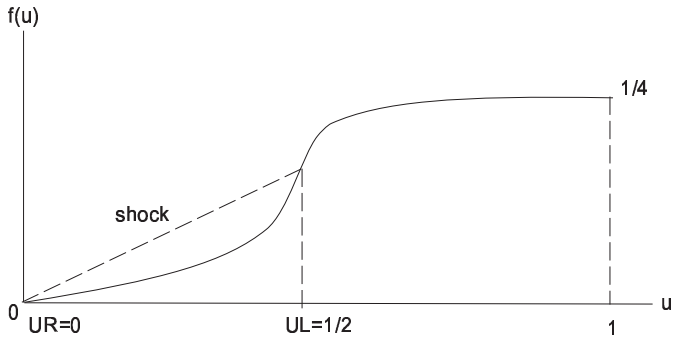

Figure 2.8: Graph of B-L flux and shock construction for first initial conditions

where

$$a(u_0) = \frac{\left(5u_0^2 - 2u_0 + 1\right)\left(8u_0 - 4u_0^2 - 10u_0 - 2\right)}{\left(5u_0^2 - 2u_0 + 1\right)^2}$$

Hence

$$\frac{dx}{dt} = a(u_0) = \frac{8u_0 - 8u_0^2}{\left(5u_0^2 - 2u_0 + 1\right)^2}$$

The characteristics are now

$$x = \left(\frac{8u_0 - 8u_0^2}{5u_0^2 - 2u_0 + 1}\right)^2 t + x_0 \qquad (2.25)$$

We can substitute the initial conditions into equation (2:25), giving

$$x = \begin{cases} \frac{32}{25}t & x_0 = 0 \quad (\textit{leaving the } t \textit{ - axis}) \\ x_0 & x_0 > 0 \quad (\textit{leaving the } x \textit{ - axis}) \end{cases}$$

At $x = t$ 2

and we have the shock speed

$$\frac{dx_s}{dt} = \frac{f_R \; i \; f_L}{u_R \; i \; u_L} = \frac{0 \; i \; \left(\frac{1}{4} \right)^2 \; i \; \left(\frac{1}{4} \right)^2}{\frac{1}{4} + \frac{1}{4} \; 1 \; i \; \frac{1}{2}} = \frac{8}{5}$$

For this initial condition we always get a shock, see figure (2.8). By looking at this

Evaluating the characteristics in the x,t plane for all $t > 0$, we obtain (as before)

$$x = \left(\frac{8u_0 - 8u_0^2}{5u_0^2 - 2u_0 + 1} \right)^2 t + x_0 \tag{2.26}$$

This time we get not only a shock but also a fan (see Figure 2.10) because we

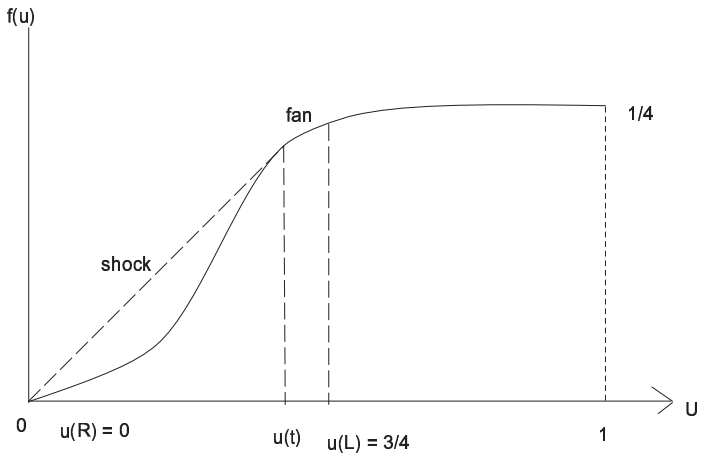

Figure 2.10: Buckley-Leverett equation for example 2

cannot connect the points $(0;0)$ and $(\frac{3}{4}; f(\frac{3}{4}))$ by a straight line, and satisfy the entropy condition see equation (2.65). Instead let u_T the value of u corresponding to the tangent from $(0;0)$ to the curve. To evaluate u_T, we proceed as follows:

The slope of curve at u_T must equal slope of tangent at u_T, therefore

$$f'(u_T) = \frac{f(u_T) - 0}{u_T - 0} \tag{2.27}$$

which leads to

$$\left(\frac{8u_T - 8u_T^2}{5u_T^2 - 2u_T + 1} \right)^2 = \frac{u_T^2 + \frac{1}{4}(1 - u_T)^2}{u_T} \tag{2.28}$$

Therefore u_T is given by equation (2.28). This is a non-linear equation for u_T. In order to use Newton's method to solve equation (2.28) we re-arrange it to obtain in the form $F(u_T) = 0$ to, where $F(u_T)$ is

$$F(u_t) = \left(\frac{8u_T - 8u_T^2}{5u_T^2 - 2u_T + 1}\right)^{\frac{1}{2}} - \frac{u_T^2 + \frac{1}{4}(1 - u_T)^{\frac{1}{2}}}{u_T} \tag{2.29}$$

The method is described in terms of a sequence, using the Newton formula

$$x_{n+1} = x_n - \frac{F(x_n)}{F'(x_n)} \tag{2.30}$$

By starting with an initial guess of $\frac{1}{2}$, we obtain the value of u_T after 5 iterations where $u_T = 0.617403$. The actual form of fan is beyond the scope of this work, so it is just sketched.

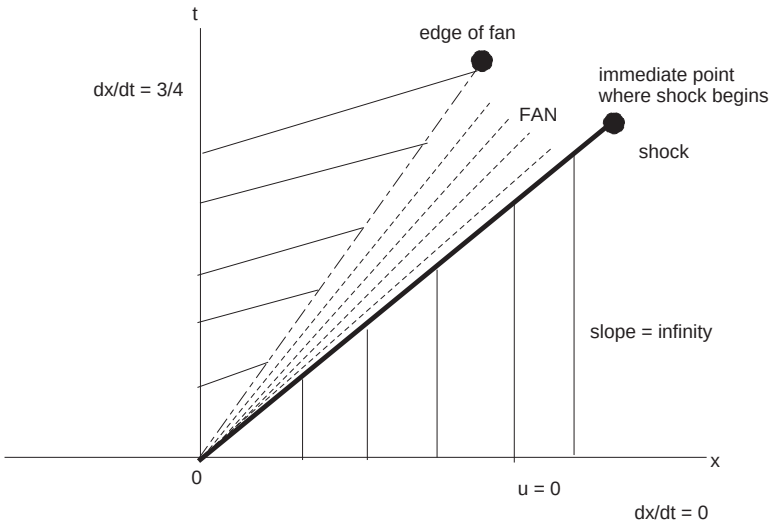

Figure 2.11: Sketch of characteristic diagram for the Buckley-Leverett equation

Chapter 3

Classical numerical schemes

Consider the general form of the hyperbolic conservation law given by equation (2.1). In our case the two non-linear equations used are the Burgers and the Buckley-Leverett equations. The flux of the equations are given by $f(u) = {}^{1}$

3.2 Lax-Friedrichs

The Lax Friedrichs scheme is first order accurate in both space and time, and the stability region is defined by $\bar{a}\frac{\Delta t}{\Delta x}\bar{} \cdot 1$. The picture on the right of figure (3.1)

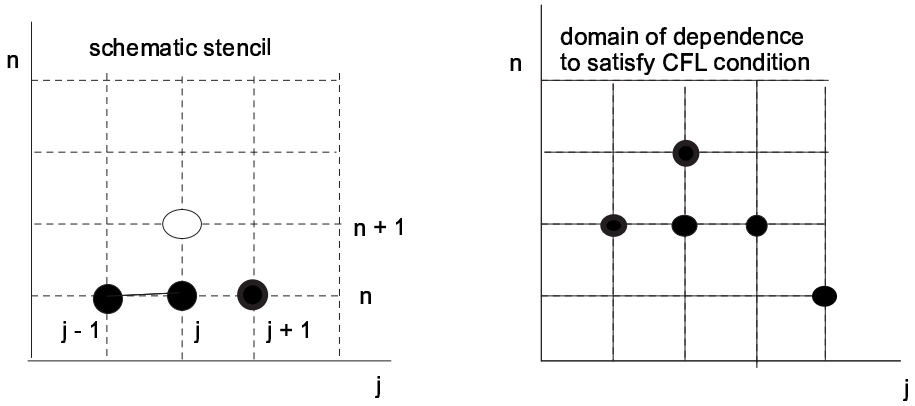

and

$$h^n_{j\,i\,\frac{1}{2}} = \frac{1}{2}\left(\frac{1}{2}u^2_{j\,i\,1} + \frac{1}{2}u^2_j\right) - \frac{\Delta x}{2\Delta t}\left(u^n_j - u^n_{j\,i\,1}\right) \tag{3.6}$$

We can now write down the Lax-Friedrichs conservative finite difference scheme for solving the conservation law for the Burgers equation in its conservative form by substituting equation (3.5) and (3.6) into equation (3.1). Doing this we obtain.

$$u^{n+1}_j = u^n_j - \frac{\Delta t}{\Delta x}\left[\left(\frac{1}{2}\left(\frac{1}{2}u^2_j + \frac{1}{2}u^2_{j+1}\right) - \frac{\Delta x}{2\Delta t}\left(u^n_{j+1} - u^n_j\right)\right)\right.$$

$$\left. - \left(\frac{1}{2}\left(\frac{1}{2}u^2_{j\,i\,1} + \frac{1}{2}u^2_j\right) - \frac{\Delta x}{2\Delta t}\left(u^n_j - u^n_{j\,i\,1}\right)\right)\right] \tag{3.7}$$

and simplifying equation (3.7) gives

$$u^{n+1}_j = u^n_j - \frac{\Delta t}{4\Delta x}\left(u^2_{j+1} + u^2_{j\,i\,1}\right) + \frac{1}{2}\left(u^n_{j+1} + u^n_{j\,i\,1}\right) \tag{3.8}$$

By substituting the flux of the Buckley-Leverett equation into equation (3.4), we get

$$h^n_{j+\frac{1}{2}} = \frac{1}{2}\left[\frac{u^2_j}{u^2_j + \frac{1}{4}(1 - u_j)^2} + \frac{\Delta}{}\right.$$

form by substituting equation (3.9) and (3.10) into equation (3.1), leads to

$$u_j^{n+1} = u_j^n - \frac{\Delta t}{\Delta x}\left[\frac{1}{2}\left(\frac{u_j^2}{u_j^2 + \frac{1}{4}(1-u_j)^2} + \frac{u_{j+1}^2}{u_{j+1}^2 + \frac{1}{4}(1-u_{j+1})^2}\right) - \frac{\Delta x}{2\Delta t}\left(u_{j+1}^n - u_j^n\right)\right]$$

$$- \left[\frac{1}{2}\left(\frac{u_{j-1}^2}{u_{j-1}^2 + \frac{1}{4}(1-u_{j-1})^2} + \frac{u_j^2}{u_j^2 + \frac{1}{4}(1-u_j)^2}\right) - \frac{\Delta x}{2\Delta t}\left(u_j^n - u_{j-1}^n\right)\right] \qquad (3.11)$$

and simplifying equation (3.11) gives

$$u_j^{n+1} = u_j^n - \frac{\Delta t}{2\Delta x}\left[\frac{u_{j+1}^2}{u_{j+1}^2 + \frac{1}{4}(1-u_{j+1})^2} - \frac{u_{j-1}^2}{u_{j-1}^2 + \frac{1}{4}(1-u_{j-1})^2}\right] + \frac{1}{2}\left(u_{j+1}^n + u_{j-1}^n\right) \qquad (3.12)$$

The Lax-Friedrichs scheme has now been written in its conservative form for the Burgers and the Buckley-Leverett equations.

3.3 First order upwind

The first order upwind scheme is also first order accurate in both space and time, but the scheme is only stable for the interval $0 \cdot a\frac{\Delta t}{\Delta x} \cdot 1$ for ($a > 0$), or $-1 \cdot a\frac{\Delta t}{\Delta x} \cdot 0$ for ($a < 0$).

The picture on the right of figure (3.2) also shows the domain of dependence. If $a\frac{\Delta t}{\Delta x}$ is slope of AB then the CFL condition is satisfied because AB lies in the stencil of the scheme, whilst the line AC is a violation of the CFL condition, lying outside the domain of dependence. The numerical flux function is

For $h_{j\,i\,\frac{1}{2}}$, we obtain

$$h_{j\,i\,\frac{1}{2}} = \begin{cases} \frac{1}{2}u^2_{j\,i\,1} & v_{j\,i\,\frac{1}{2}} > 0 \\ \frac{1}{2}u^2_{j} & v_{j\,i\,\frac{1}{2}} < 0 \end{cases} \tag{3.16}$$

where

$$v_{j\,i\,\frac{1}{2}} = \begin{cases} \frac{\Delta t}{\Delta x}\frac{1}{2}(u_j + u_{j\,i\,1}) & u_{j\,i\,1} \neq u_j \\ \frac{\Delta t}{\Delta x}u_{j\,i\,1} & u_{j\,i\,1} = u_j \end{cases}$$

We can now write the first order upwind scheme for solving the conservation law, for the Burgers equation in its conservative form by substituting equation (3.15) and (3.16) into equation (3.1), which gives rise to

$$u^{n+1}_j = u^n_j - \left[\frac{\Delta t}{\Delta x}\right] equation(3.15) - equation(3.16) \tag{3.17}$$

Introducing the Buckley-Leverett flux into the first order upwind scheme, for

line AC violates the CFL condition, by lying outside the domain of dependence.

The numerical flux function can be written as

$$h_{j+\frac{1}{2}} = \frac{1}{2}\left(f_{j+1} + f_j\right) - v_{j+\frac{1}{2}}\left(f_{j+1} - f_j\right) \tag{3.21}$$

Substituting the Burgers flux gives rise to

$$h_{j+\frac{1}{2}} = \frac{1}{2}\left(\frac{1}{2}u_{j+1}^2 + \frac{1}{2}u_j^2\right) - v_{j+1}$$

where $v_{j\,i\,\frac{1}{2}}$ and $v_{j+\frac{1}{2}}$ for this scheme are as in the first order upwind scheme. We can now write the Lax-Wendroff scheme for solving the conservation law, for the Burgers and the Buckley-Leverett equations may be written as

$$u_j^{n+1} = u_j^n - \frac{\Delta t}{\Delta x}\left[equation(3.22) - equation(3.23)\right] \tag{3.26}$$

and

$$u_j^{n+1} = u_j^n - \frac{\Delta t}{\Delta x}\left[equation(3.24) - equation(3.25)\right] \tag{3.27}$$

3.5 Warming-Beam

The Warming-Beam is also a second order accurate numerical scheme, but the scheme is only stable for the interval $0 \cdot a\frac{\Delta t}{\Delta x} \cdot 2$.

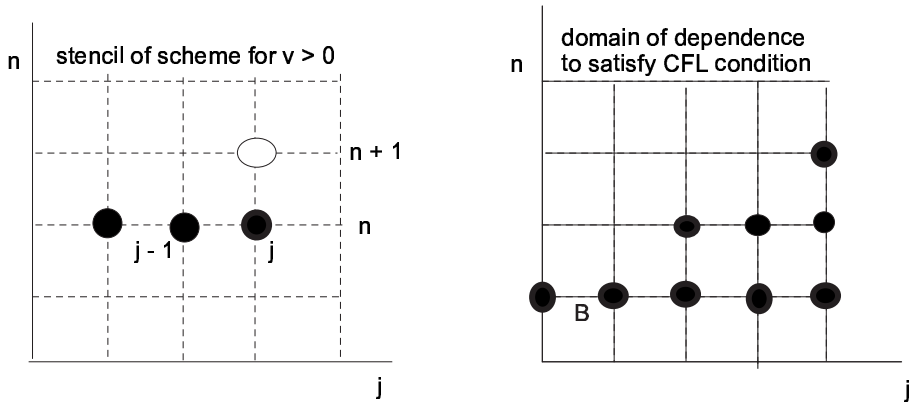

Figure 3.4: Stencils for the Warming-Beam scheme

The picture on the right of figure (3.4) shows the domain of dependence for this numerical scheme. If $a\frac{\Delta t}{\Delta x}$ is the slope of AB then the CFL condition is satisfied

because AB lies in the stencil of the scheme, whilst the line AC violates the CFL condition, by lying outside the domain of dependence. The numerical flux function can be written as

$$h_{j+\frac{1}{2}} = \begin{cases} \frac{1}{2}\left(3f_j - f_{j-1}\right) - \frac{1}{2}v_{j-\frac{1}{2}}\left(f_j - f_{j-1}\right) & v_{j+\frac{1}{2}} > 0 \\ \frac{1}{2}\left(3f_{j+1} - f_{j+2}\right) - \frac{1}{2}v_{j+\frac{3}{2}}\left(f_{j+2} - f_{j+1}\right) & v_{j+\frac{1}{2}} < 0 \end{cases} \tag{3.28}$$

and

$$h_{j-\frac{1}{2}} = \begin{cases} \frac{1}{2}\left(3f_{j-1} - f_{j-2}\right) - \frac{1}{2}v_{j-\frac{3}{2}} \end{cases}$$

and

the TVD (total variation diminishing) property, which the original problem satisfies. The total variation $TV = \sum j u_{j+1}^n - u_j^n j$ and the D means it is decreasing in time (within). The introduction of flux limiters can be added to the Lax Wendroff and Warming-Beam schemes in order to make it TVD and therefore non-oscillatory. I have not pursued limiters for the finite difference methods here for the lack of time

respectively. Examination of these two equations by using Fourier Transforms [12], shows the schemes to be of a non-dispersive nature, due to the waves travelling at the same speed as of those in equation (1.1). The CFL number $a\frac{\Delta t}{\Delta x}$ is positive and at most 1, so when $D > 0$ the amplitudes of the waves are damped with the higher wave numbers being affected more severely. Therefore we can conclude that the Lax- Friedrichs and first order upwind schemes are dissipative. By looking at equations (3.31) and (3.32) we can clearly see that the coefficient for the Lax- Friedrichs scheme has a much larger factor than of the first order upwind scheme, so we expect the Lax-Friedrichs scheme to be much more diffusive than the first order upwind scheme.

The modified equation for the Lax-Wendroff and Warming-Beam numerical schemes can be written in the form

$$u_t + a(u)u_x = Ru_{xxx} \tag{3.33}$$

where

$$R = \frac{1}{6}\Delta x^2 \left(a^2\frac{\Delta t^2}{\Delta x^2} - 1\right) \tag{3.34}$$

and

$$R = \frac{1}{6}\Delta x^2 \left(2 - a\frac{\Delta t}{\Delta x}\right)\left(1 - a^2\frac{\Delta t^2}{\Delta x^2}\right) \tag{3.35}$$

respectively. Investigation of equation (3.33) by Fourier Transforms shows that different wave numbers are travelling at different speeds, which means that the equation is said to be dispersive. By looking at the stability region for the Lax-Wendroff scheme, we can see that R is negative, which leads to high wave numbers travelling

with slower speed than they should. As a result of this we obtain oscillations occurring to the left of a shock. Due to the comparison of clasical numerical schemes, we shall concentrate on the lower half of the stability region $0 \cdot a\frac{\Delta t}{\Delta x} \cdot 1$ for the Warming-Beam scheme. If we consider the lower half of the stability region, by looking at equation (3.35) we can see that R will always stay positive. This resulting in high wave numbers travelling with faster velocity than they should, therefore the oscillations are observed in the front of the discontinuity for the Warming-Beam scheme.

Numerical results for the application of the schemes for Burgers and the Buckley-Leverett equations will be shown in chapter 5.

Chapter 4

Discontinuous Galerkin Method

In this Chapter we describe the derivation of the Discontinuous Galerkin Method, a non-classical method, and its application to the Buckley-Leverett equation.

4.1 Basic derivation of D-G Method

Given

$$u_t + f(u)_x = 0; \qquad in \qquad (a;b) \pounds (0;T) \tag{4.1}$$

with an initial condition

$$u(x;0) = u_0(x); 8x \; 2 \; (a;b) \tag{4.2}$$

To numerically solve equations (4:1) and (4:2), we can use the Discontinuous Galerkin method to discretise in space with a Runge-Kutta method to step forward in time [4] and [5]. We shall first discretize (4:1) and (4:2) in the spatial variable x. To discretize in space we proceed as follows. For each part of the interval $(a;b)$, we set

$I_j = (x_{j-\frac{1}{2}}, x_{j+\frac{1}{2}})$ where $\Delta_j = x_{j+\frac{1}{2}} - x_{j-\frac{1}{2}}$ for $j = 1, \ldots, N$ and denote the quantity $max_{1 \le j \le N} \Delta_j$ by Δx. We use the Galerkin method for which the finite dimensional space V_h to which the approximate solution $u^h(t)$ belongs to is taken as

$$V_h = V_h^k = \{ v \in L_1(0,1) : v|_{I_j} \in P^k(I_J), j = 1, \ldots, N \}$$

where $P^k(I_j)$ denotes the space of polynomials of degree at most k in the cell (I_j). In V_h^k, the functions are allowed to have jumps at the interfaces $x_{j+\frac{1}{2}}$ which is why this method is called the Discontinuous Galerkin method. Multiply equation (4.1) by v and integrate over I_j,

$$\int_{I_j} v u_t dx + \int_{I_j} v f(u)_x dx = 0. \tag{4.3}$$

Integrating the second term by parts, gives

$$\int_{I_j} v u_t dx + \left[v f(u) \right]_{I_j} - \int_{I_j} v_x f(u) dx = 0 \tag{4.4}$$

Equation (4.4) is the weak form used for linear approximation. For each j put $u = u_0 + (x - x_{j-\frac{1}{2}})u_1$ and choose $v_0 = 1$ and $v_1 = (x - x_{j-\frac{1}{2}})$. Substituting $v_0 = 1$ into equation (4.4), yields

$$\int_{I_j} u_t dx + \left[f(u) \right]_{I_j} = 0. \tag{4.5}$$

Substituting $v_1 = (x - x_{j-\frac{1}{2}})$ into equation (4.4) we get

$$\int_{I_j} (x - x_{j-\frac{1}{2}}) u_t dx + \left[(x - x_{j-\frac{1}{2}}) f(u) \right]_{I_j} - \int_{I_j} f(u) dx = 0 \tag{4.6}$$

Equations (4:5) and (4:6) for all the j^0s can be written in a concise ODE form

$$\frac{d}{dt}u_h = L_h(u^h) \tag{4.7}$$

where u_h

4.2 Buckley-Leverett flux

Introducing the Buckley - Leverett flux into equation (4:5) gives

$$\int_{I_j} u_t dx + \left[\frac{u^2}{u^2 + \frac{1}{4}(1 - u)^2} \right]_{I_j} = 0 \tag{4.8}$$

Introducing the flux into equation (4:6) gives

$$\int_{I_j} (x - x_{j-\frac{1}{2}}) u_t dx + (x - x_{j-\frac{1}{2}}) \left[\frac{u^2}{u^2 + \frac{1}{4}(1 - u)^2} \right]_{I_j} - \int_{I_j} \left(\frac{u^2}{u^2 + \frac{1}{4}(1 - u)^2} \right) dx = 0 \tag{4.9}$$

To evaluate the first term of equation (4:8), we proceed as follows

$$\int_{x_L}^{x_R} u_t dx = \int_{I_j} \left(\frac{du_L}{dt} \acute{A}_L(x) + \frac{du_R}{dt} \acute{A}_R(x) \right) dx$$

$$= \frac{du_L}{dt} \int_{x_L}^{x_R} \left(\frac{x_R - x}{x_R - x_L} \right) dx + \frac{du_R}{dt} \int_{x_L}^{x_R} \left(\frac{x - x_L}{x_R - x_L} \right) dx$$

By integrating we obtain

$$\int_{x_L}^{x_R} u_t dx = \frac{du_R}{dt} \frac{1}{x_R - x_L} \left[\frac{1}{2} - x - x_L)^{\cent 2} \right]_{x_L}^{x_R} + \frac{du_L}{dt} \frac{1}{x_R - x_L} \left[\frac{1}{2} - x_R - x)^{\cent 2} \right]_{x_L}^{x_R}$$

Substituting in the limits we obtain

$$\int_{x_L}^{x_R} u_t dx = \frac{du_R}{dt} \frac{1}{2} - x_R - x_L^{\cent} + \frac{du_L}{dt} \frac{1}{2} - x_L - x_R^{\cent}: \tag{4.10}$$

To evaluate the second term of equation (4

$$\left[\frac{\partial u}{\partial t}\right]_j = \frac{1}{\Delta x_j}\left(f\left(u\left(x_{j+\frac{1}{2}}, t\right)\right) - f\left(u\left(x_{j-\frac{1}{2}}, t\right)\right)\right)$$

Replacing the non-linear flux $f\left(u\left(x_{j+\frac{1}{2}}, t\right)\right)$ by a numerical flux which depends on two values of u_h at the point $\left(x_{j+\frac{1}{2}}, t\right)$, this is given by

$$h(u)_{j+\frac{1}{2}}(t) = h\left(u(x^{-}_{j+\frac{1}{2}}; t), (u(x^{+}_{j+\frac{1}{2}}; t)\right)$$

By using a monotone numerical flux, we should achieve high-order accuracy while keeping their stability and convergence properties. A monotone flux is one which satisfies the following properties listed below.

- If it is locally Lipschitz and consistent with the flux $f(u)$, for example $h(u; u) = f(u)$.
- If it is a nondecreasing function of its first argument, and a nonincreasing function of its second argument

An example of a numerical flux which satisfies the above properties is the Local Lax-Friedrichs flux, 7ive6 by

$$i\frac{1}{2}\left(\frac{u^{+2}_{j\,i\,\frac{1}{2}}}{u^{+2}_{j\,i\,\frac{1}{2}}+\frac{1}{4}}1\,i\,u^{+}_{j\,i\,\frac{1}{2}}\right)^{2}\;i\;\frac{1}{2}C\left(u^{+}_{j+\frac{1}{2}}\,i\,u^{i}_{j+\frac{1}{2}}\right)+\frac{1}{2}C\left(u^{+}_{j\,i\,\frac{1}{2}}\,i\,u^{i}_{j\,i\,\frac{1}{2}}\right)$$

To evaluate the first term of equation (4:9), we proceed as follows

$$\int_{x_L}^{x_R}(x\,i\,x_L)u_t dx=\int_{x_L}^{x_R}(x\,i\,x_L)\left(\frac{du_L}{dt}\acute{A}_L(x)+\frac{du_R}{dt}\acute{A}_R(x)\right)dx$$

$$=\frac{du_L}{dt}\int_{x_L}^{x_R}(x\,i\,x_L)\left(\frac{x_R\,i\,x}{x_R\,i\,x_L}\right)dx+\frac{du_R}{dt}\int_{x_L}^{x_R}(x\,i\,x_L)\left(\frac{x\,i\,x_L}{x_R\,i\,x_L}\right)dx$$

By integrating we obtain

$$\int_{x_L}^{x_R}(x\,i\,x_L)u_t dx=\frac{du_R}{dt}\frac{1}{x_R\,i\,x_L}\left(\frac{1}{3}\mathrm{i}\,x\,i\,x_L\right)^{3}_{x_L}+\frac{du_L}{dt}\frac{1}{x_R\,i\,x_L}\left(\frac{x_R x^2}{2}\,i\,x_L x_R x\,i\,\frac{x^3}{3}+\frac{x_L x^2}{2}\right)^{x_R}_{x_L}$$

hence

$$\int_{x_L}^{x_R}(x\,i\,x_L)u_t dx=\frac{du_R}{dt}\left(\frac{1}{3}\mathrm{i}\,x_R\,i\,x_L\right)^{2}+\frac{du_L}{dt}\frac{1}{x_R\,i\,x_L}\left(\frac{1}{6}x_R^3\,i\,\frac{1}{2}x_L x_R^2\,i\,\frac{1}{6}x_L^3+\frac{1}{2}x_R x_L^2\right)$$

To evaluate the second term of equation (4:9), we treat this term in the same way as we did previously for the second term in equation (4:8). By doing this we obtain

$$(x\,i\,x_{j\,i\,\frac{1}{2}})f\left(\mathrm{i}\,u\right)^{x_{j+\frac{1}{2}}}_{j\,i\,\frac{1}{2}}=\left(\mathrm{i}\,x_{j+\frac{1}{2}}\,i\,x_{j\,i\,\frac{1}{2}}\right)\left(f\left(\mathrm{i}\,u_{j+\frac{1}{2}}\right)\right)$$

Applying the Local-Lax Friedrichs flux to this term yields

$$h^{LLF}=\frac{1}{2}\left(\mathrm{i}\,x_{j+\frac{1}{2}}\,i\,x_{j\,i\,\frac{1}{2}}\right)\left(\frac{u^{i\,2}_{j+\frac{1}{2}}}{u^{i\,2}_{j+\frac{1}{2}}+\frac{1}{4}}1\,i\,u^{i}_{j+\frac{1}{2}}\right)^{2}+\frac{1}{2}\left(\mathrm{i}\,x_{j+\frac{1}{2}}\,i\,x_{j+\frac{1}{2}}\right)\left(u^{+2}_{j+}{}^{11}\right.$$

$$i\frac{1}{2}\,x_{j+\frac{1}{2}}\;i\;x_{j\,i\,\frac{1}{2}}\;\Big\¢i\frac{1}{3}\,x_{j+\frac{1}{2}}\;i\;x_{j\,i\,\frac{1}{2}}\;\Big\¢_2\¢^{\mu}\;u^{+}_{j+\frac{1}{2}}\;i\;u^{j}_{j+\frac{1}{2}}\;\Big\¶$$

We are now left with the final term in equation (4:9). To integrate this we use Gaussian Quadrature. To evaluate Lu

Solving equations (4:12) and (4:13) simultaneously yields

$$\frac{du_L}{dt} = \frac{C \¤ RHS1 \ ¡ \ A \¤ RHS2}{B \¤ C \ ¡ \ A \¤ D} \tag{4.14}$$

and

$$\frac{du_R}{dt} = \frac{RHS1}{A} \ ¡ \ B\frac{(RHS1 \ ¡ \ A \¤ RHS2)}{A(B \¤ C \ ¡ \ A \¤ D)} \tag{4.15}$$

We can now apply the TVD-Runge-Kutta to discretise our ODE system in time [2]. If $\{t^n\}_{n=0}^{N}$ is a partition of $[0;T]$ and $\Delta t^n = t^{n+1} \ ¡ \ t^n; n = 0;¢¢¢;N \ ¡ \ 1$, then our time marching algorithm reads as follows:

² Set $u_h^0 = u_h^n$;

² For $n = 0;¢¢¢;N \ ¡ \ 1$ compute u_h^{n+1} from u_h^n as follows:

1 Set $u_h^0 = u_h^n$;

2 for $i = 1;¢¢¢;k+1$ compute the intermediate functions:

$$u_h^i = \tilde{A}^{\,iX^{1}}_{l=0} \®_{il}u_h^l + \¯_{il}\Delta t^n L_h\{u_h^l\}^{¢}\ !; \tag{4.16}$$

3 set $u_h^{n+1} = u_h^{(k+1)}$.

where $L_h\{u_h^l\}^{¢}$ is given by equations (4:14) and (4:15). In equation (4:16) we take k to equal one, where $\®_{il}$ and $\¯_{il}$ are the Runge-Kutta time discretisation parameters.

Chapter 5

Numerical Results

Numerical experiments were performed using five di□erent numerical schemes. The schemes used are the first order upwind, Lax-Friedrichs, Lax- Wendro□, Warming-Beam and the Runge-Kutta Discontinuous Galerkin method. Unfortunately we could not get the RKDG program to work, so used one kindly made available by Paul Jelfs. The Burgers and Buckley-Leverett equations were used,

$$u_t + \tilde{A}\frac{1}{2}$$

5.1 Burgers initial data 1

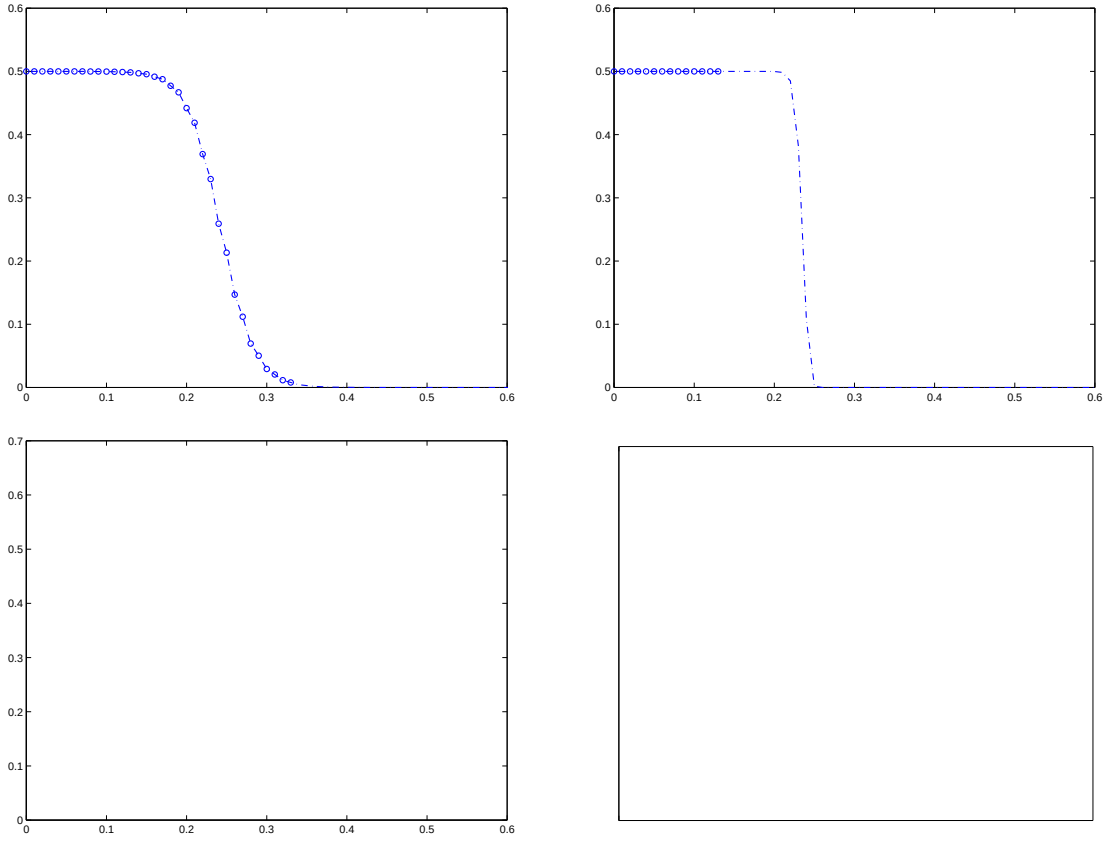

Figure 5.1: Graphs of schemes for Burgers' initial data 1 points

The solution for this data describes a shock which is propagating in the positive x-direction, with a speed of 0.25. We can compare the behaviour of the numerical schemes, since the analytic solution is known. Figures (5:1) and (5:2) were plotted using a step size $\Delta x = 0{:}01$ and a time step $\Delta t = 0{:}009$, with a number of 100 timesteps used for figure (5:1). At this particular time point the shock has moved to $x = 0{:}225$ from its initial position. By analysing fig (5:1) we can clearly see that the Lax-Friedrichs and the first order upwind schemes have introduced numerical

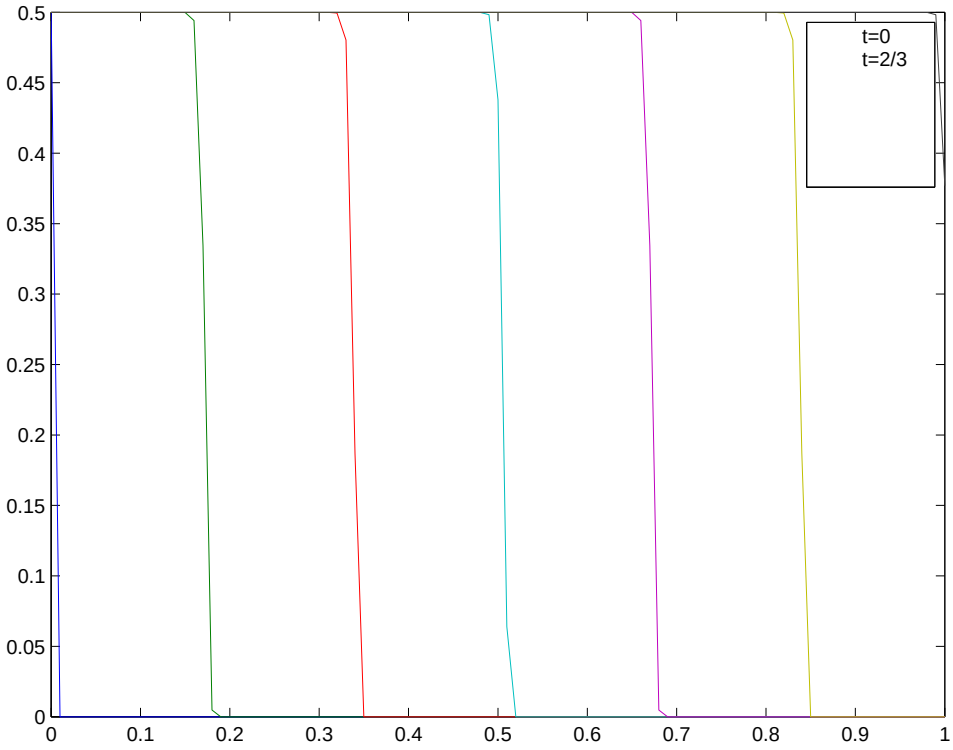

Figure 5.2: Graph of RKDG method for Burgers equation with initial data 1

di□usion (smearing). The smearing for the Lax-Friedrichs scheme is much more severe than of the first order upwind scheme, this being a direct feature of the truncation error terms of these schemes (see Chapter 3), whilst the Lax-Wendro□ and Warming-Beam schemes are much more accurate at capturing the shock. The Lax-Wendro□ scheme produces spurious oscillations to the left of the shock and the Warming-Beam scheme creates oscillations to the right of the shock, as can be seen by looking at figure (5.1). Finally by looking at figure (5:2) we can see that the RKDG method does not create oscillations, due to the use of the TVD Runge-Kutta to march forward in time. However, there is a subtle smearing if we look at the time intervals provided on the graph.

5.2 Burgers initial data 2

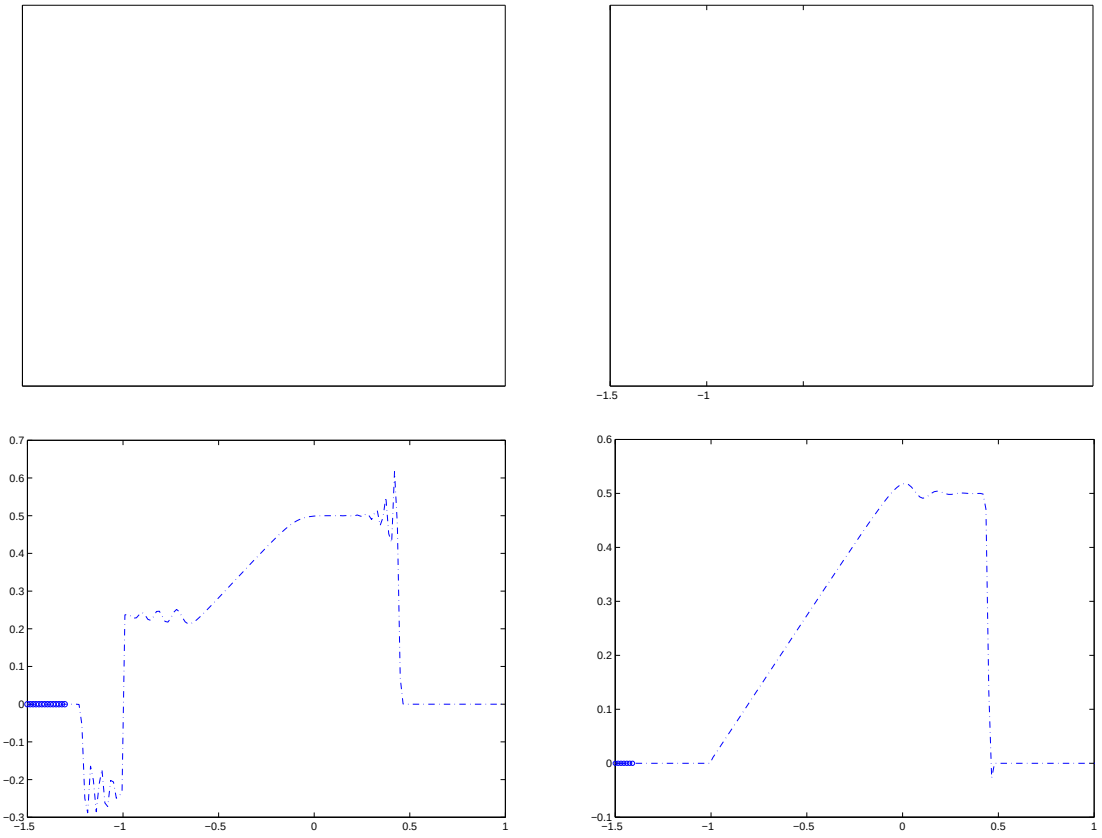

Figure 5.3: Graphs for Burgers' initial data 2 points

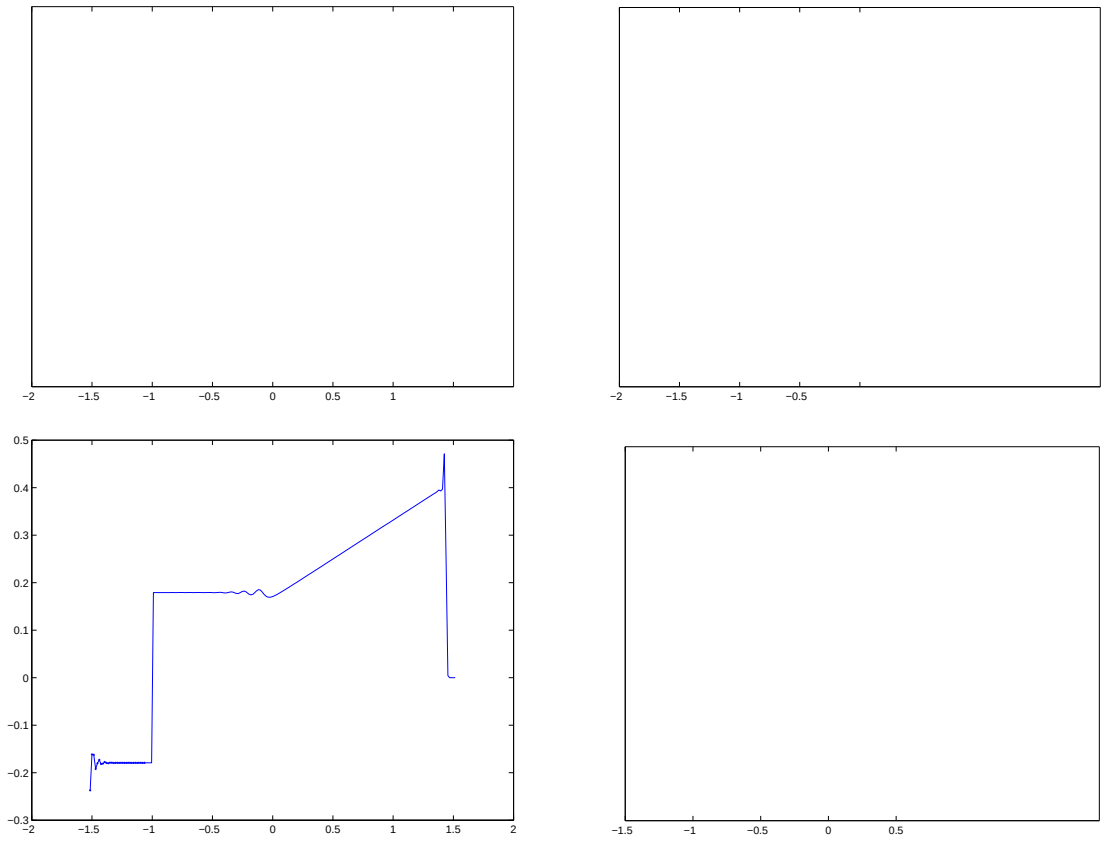

Figure 5.4: Graphs for Burgers' initial data 2 points

which has influenced the accuracy of the scheme compared to the analytical solution. The first order upwind scheme has behaved somewhat better, with better accuracy than of the Lax-Friedrichs scheme. The Lax-Wendro□ and Warming-Beam schemes are the most accurate of the four classical schemes, but the overall phase shape is quite poor, due to introduction of oscillations which are present behind and front of the discontinuities, respectively. The behaviour to the left of the fan for the Lax-Wendro□ scheme is due to entropy violation. Figure (5.4) was plotted using a step size $\Delta x = 0.02$ and a time step of $\Delta t = 0.03$, with 200 timesteps,

Figure 5.5: Graph for Lax Wendroff scheme with initial data (5.3)

giving a location time of 6. At this time the expansion fan and the shock are combined together. By looking at figure (5.4), we can clearly see that by moving forward in time, the initial square wave has been damped, this being a feature of the shock and fan combining together. Once again the Lax-Friedrich scheme is the most dissipative in comparison to the first order upwind scheme, both of the schemes giving poor resolution to discontinuities. Although the Lax-Wendroff and Warming-Beam schemes are creating oscillations, the position of the final location of the shock are most accurate.

If we change initial data 2 and use the initial conditions

$$u(x,0) = \begin{cases} 0.5 & x < -1 \\ 1 & -1 < x < 0 \\ 0.5 & x > 0 \end{cases} \tag{5.3}$$

we do not obtain the entropy violation as occurred in figures (5.3) and (5.4) for the Lax-Wendroff scheme. Figure (5.5) was plotted using a step size $\Delta x = 0.0125$ and a time step of $\Delta t = 0.009$, with 200 timesteps. By looking at this figure we can clearly see that the problem we faced earlier has been resolved. The graph shows that at the discontinuities, the oscillations are behind the shock and the expansion fan.

5.3 Buckley - Leverett initial data 1

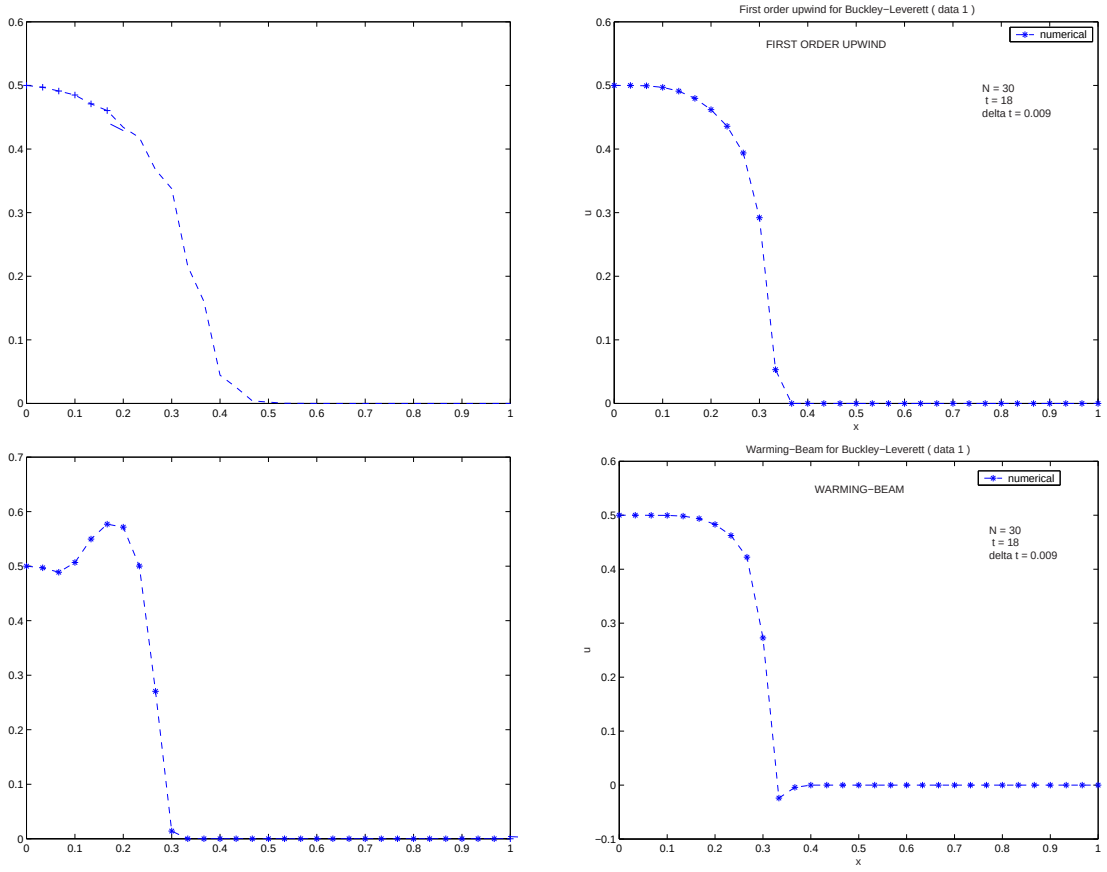

Figure 5.6: Graphs for Buckley-Leverett using initial data 1

of these type of second order numerical schemes. By looking at figure (5.7), we can see that the waves for the RKDG method seem to be travelling way too slow. However by extracting the behaviour from these results, we can visualise that there are no oscillations present due to the built in TVD property.

5.4 Buckley - Leverett initial data 2

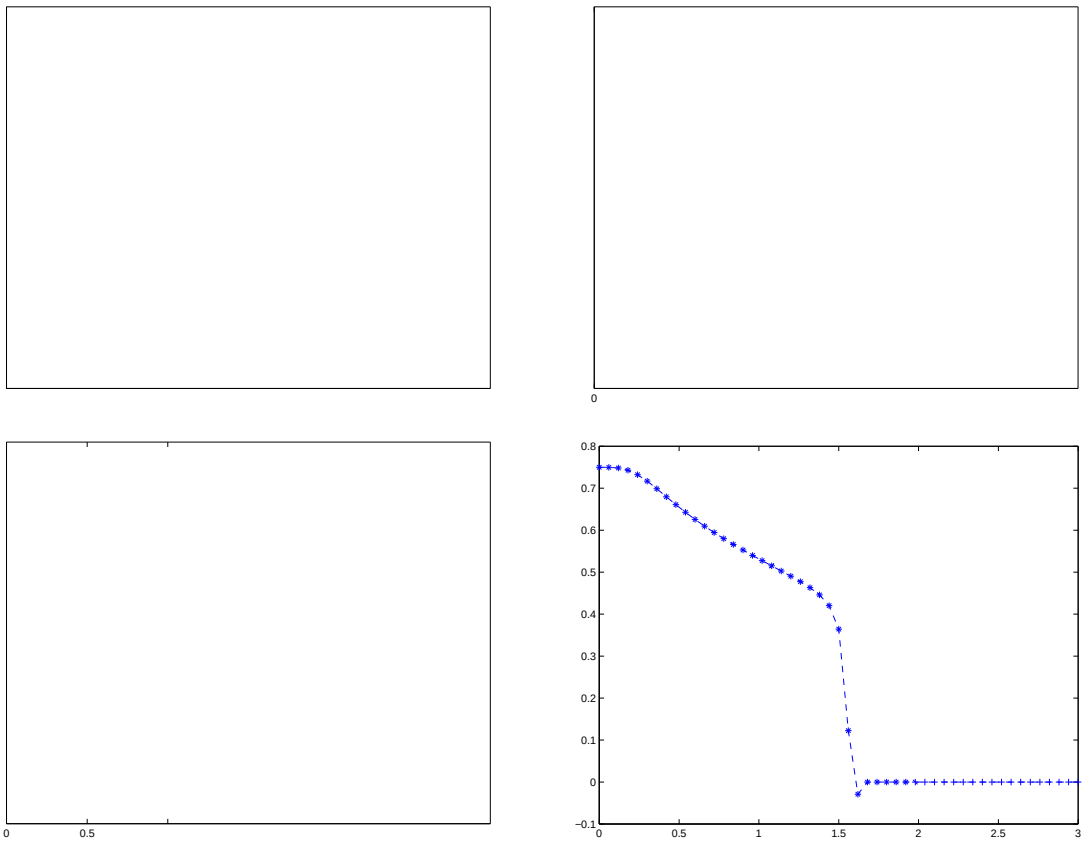

Figure 5.8: Graphs for Buckley-Leverett using initial data 2

This initial data generates a fan and a shock conbination. Figures (5.8) and (5.9) was plotted using a step size $\Delta x = 0.06$ and a time step $\Delta t = 0.009$, where the

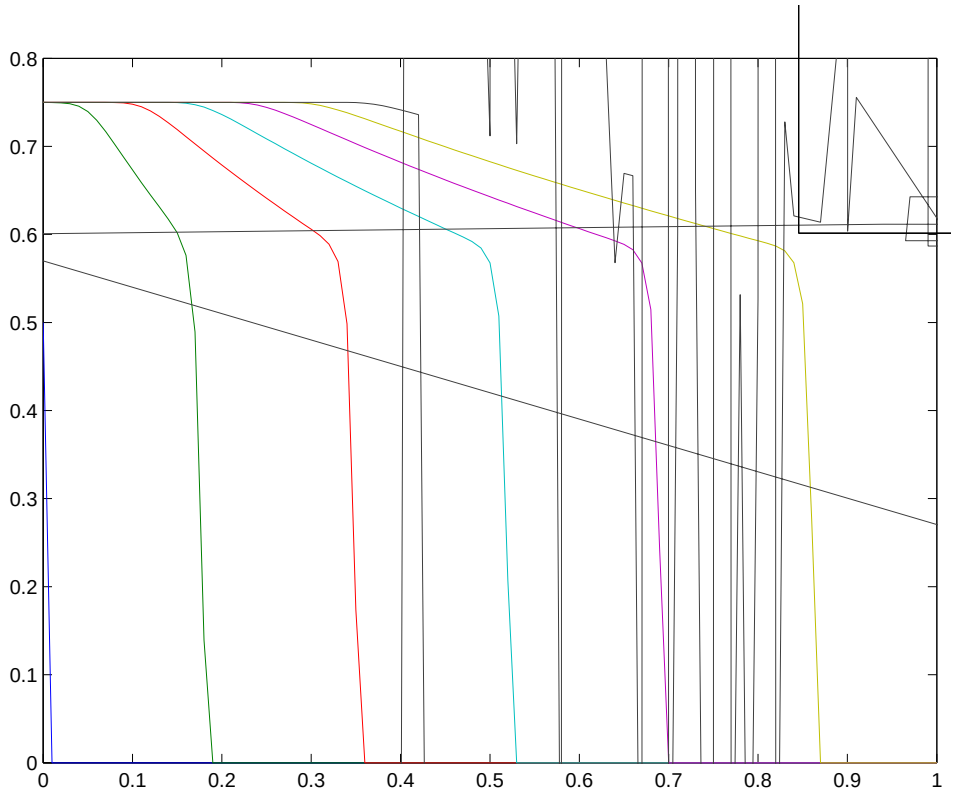

Figure 5.9: RKDG for Buckley-Leverett initial data 2

number of timesteps is 100 for figure (5.8). From the results obtained in figure (5.8) we can clearly see that the Lax-Friedrichs scheme is yet again the most diffusive, in comparison to the first order upwind scheme.

The Lax-Wendroff scheme for this initial data seems not to have produced any visible oscillations to the left of the shock. This is most probably due to the combination of the fan and the shock combining together at left of the shock, where the fan is damping the oscillations that are produced by the shock, therefore resulting with no visible oscillations to the left of the shock. By looking at the Warming-Beam scheme we can clearly see that oscillations are still present to the right of the shock

as initially expected. By looking at figure (5:9) we can see that the second order RKDG method has not produced any oscillations, although there is slight evidence of smearing, even though the speed of the waves are yet again moving way too slow.

Chapter 6

Conclusion

In this dissertation we have studied the effects of four classical schemes on the Burgers and Buckley-Leverett equations. The schemes are first order upwind, Lax-Friedrichs, Lax-Wendroff and Warming-Beam, found that the the Lax-Friedrichs and the first order upwind schemes are very diffusive, this being a common feature for first order accurate schemes. The reason for this type of dissipative behaviour is an artefact of the terms in the truncation error for these schemes.

The Lax-Wendroff, Warming-Beam and the RKDG method are second order accurate schemes, and it is a well known fact that second order accurate numerical schemes produce oscillations at discontinuities. The Lax-Wendroff scheme is shown to produce oscillations to the left of the discontinuities, except for initial data 2 for the Buckley-Leverett equation, where we had the fan and shock combination. The Warming-Beam scheme has produced oscillations to the right of the shock for all the cases considered. However the oscillations for the Lax-Wendroff and Warming-Beam schemes can be suppressed by using limiters, although that has not been done

Bibliography

[1] R. Ansorge, "Mathematical Models of Fluiddynamics An Introduction", WILEY-VCH GmbH and co. KGaA, (2003).

[2] E.B. Becker, G.F. Carey and J.T. Oden. "finite elements: an introduction", Prentice-Hall, New Jersey, (1981).

[3] W. Cheney and D. Kincaid, "numerical mathematics and computing", Brooks/Cole

[12] P.K Sweby, "Numerical Solution of Conservation Laws" Lecture notes, University of Reading (2002).

[13] P.K Sweby, "Theory of Di□erential equations" Lecture notes, University of Reading (2002).

[14] A.J. Wathen, "Moving finite elements and reservoir modelling" PhD Thesis, Department of Mathematics, University of Reading , (1984).